Vibration Comparison Between Conventional and Hybrid Angular Contact Bearings

Kelsen E. LaBerge [1]

[1] *Propulsion Division, U. S. Army Research Laboratory, 21000 Brookpark Rd, MS 23-3, Cleveland, OH 44135, U.S.A.*

Abstract

Within the rotorcraft industry, there is always a goal to increase the power density of the powertrain. One technology available that could potentially have a large impact on power density is hybrid bearings (ceramic rolling elements with steel races). With a density that is approximately 40% that of steel, silicon nitride rolling elements offer a significant weight savings, particularly in the case of larger bearings. However, prior to implementing hybrid bearings in rotorcraft, there must be a high confidence that damage can be detected, preferably utilizing currently installed health and usage monitoring systems. This initial study compares the vibration signatures of a faulted conventional bearing with those of a hybrid bearing. Faults were seeded into the inner races of both hybrid and conventional angular contact bearings using a Rockwell hardness indenter. The tests discussed were run under axial loading such that both the hybrid and conventional bearings experienced approximately the same contact stress. Both healthy and faulted vibration data was obtained and is compared here in an effort to understand the difference in fault vibration between the two types of bearings.

Keywords: bearings, vibration, hybrid bearings, diagnostics.

Introduction

The U.S. Army has long strived to reduce drive system weight and increase the power density of its helicopter fleet [1]. Recently, in an effort to enable helicopter manufactures to investigate weight saving technologies, the Army has held several cost-share programs such as the Future Advanced Rotorcraft Drive System program, which strives to increase the power density of Army platforms by 55 percent. Generally speaking, these programs are aimed at implementing new technologies into current Army platforms as new platform programs are rare.

One weight saving technology available is hybrid and fully ceramic bearings. While fully ceramic bearings would provide the greatest weight savings, they pose some challenges when it comes to interfacing with shafts and bearing housings, in particular a difference in the coefficient of thermal expansion. With steel raceways, hybrid bearings pose a weight savings while reducing issues where thermal expansion differences are concerned. The reduced density of ceramic rolling elements (40 percent the density of steel in the case of silicon nitride) also improves bearing load capacity at higher rotational speeds, by reducing centrifugal effects [2]. While these benefits of hybrid bearings may lead one to believe that they are an obvious improvement over conventional steel rolling element bearings, there are also potential drawbacks.

One of these drawbacks is the generation of ceramic debris. Likely the most reliable indicator of damage in a gearbox is the collection of ferrous debris on an installed magnetic chip detector or potentially even an inline inductance type debris monitor. However, neither of these methods is capable of detecting ceramic particles suspended in the oil. Several

researchers have worked on alternate methods of detecting ceramic debris in oil such as the ultrasonic sensor discussed in [3]. While ceramic debris detection is of importance, it is not the focus of this particular effort.

Perhaps the most useful method of damage detection in hybrid bearings would be one in which currently installed HUMS vibration sensors could be used. This would allow the manufacturer to potentially go to hybrid bearing alternatives without requiring a change in diagnostic hardware. Unfortunately, while there have been many papers discussing fault detection using the vibration of conventional bearings, there has been little work in the area of hybrid bearing diagnostics. A vibration comparison between conventional and hybrid bearings with silicon nitride rolling elements was performed in [4], however, it focused on general vibration characteristics of the bearings under healthy run conditions. A similar study was performed later for fully ceramic bearings in [5]. The studies were focused on natural frequencies of the different types of bearings comparing experimental results to Hertz theory. Some work has been performed on diagnostics for hybrid and full ceramic bearings at the University of Illinois-Chicago through the use of acoustic emissions [6,7]. However, to the author's knowledge, the Army rotorcraft fleet is not equipped with these sensors.

In an effort to understand and evaluate both vibration and oil debris technics in identifying the presence of damage in hybrid bearings, a test rig was developed at the NASA Glenn Research Center in Cleveland, OH and is described in [8]. The study described here utilizes this facility to provide an initial look into comparing the vibration signals of hybrid and conventional bearings, particular in the case of high-speed applications.

Experimental Setup

The Hybrid Bearing Prognostic Test Rig at NASA's Glenn Research Center was used for this bearing study (Fig. 1). Specifics regarding the apparatus can be found in [8]. The test section of the rig is supported by two wave type journal bearings and the test bearing is cantilevered from one end with the motor driving the other. Axial and radial loading is applied by way of pneumatic load cylinders. The axial thrust load is reacted by a wave thrust bearing located between the test bearing and the adjacent support bearing. The variable speed drive motor for the rig has a capability to run up to 21,000 RPM, though rig resonances prevent running above 17,000 RPM.

The test bearing housing in this rig is fully enclosed to keep the journal bearing lubrication and test bearing lubrication separate (Fig. 2). Oil is supplied to the test bearing by 3 pressurized jets and gravity drains from the test housing, traveling through an in-line off-the-shelf inductance type oil debris sensor. This allows researchers to monitor ferrous debris removed from the test bearing including an approximate ferrous weight removed as well as the approximate particle size. The test bearing housing is instrumented with both an axial and radial high-bandwidth researcher accelerometer to monitor test bearing vibrations. Facility data is recorded continuously at 1 hz throughout testing, including axial load, oil inlet and outlet temperatures, shaft speed, etc. The specifications for the test bearings used for this study are shown in Table 1.. These bearings both have the same geometry, the only difference being the substitution of silicon nitride balls for the steel balls in the case of the hybrid.

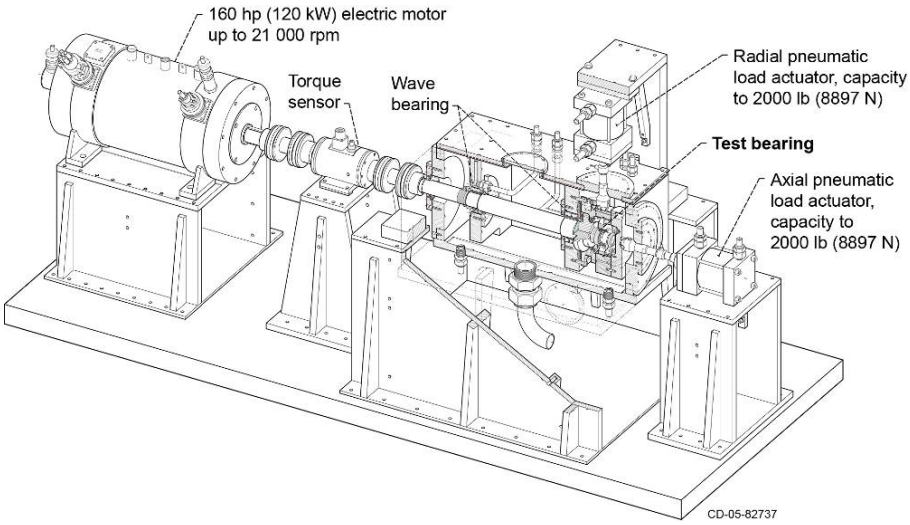

Fig. 1: NASA Hybrid Bearing Prognostics Rig diagram [8]

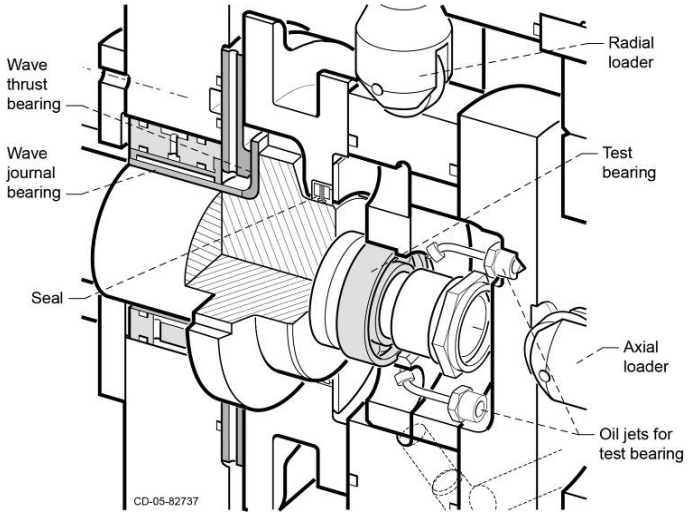

Fig. 2: Test bearing housing diagram [8]

Table 1: Test bearing specifications [9]

	Conventional	Hybrid
Inner diameter (mm)	25	25
Outer diameter (mm)	47	47
Width (mm)	12	12
Contact angle (deg)	15	15
Number of balls	14	14
Ball diameter (mm)	6.35	6.35
Ball material	Steel	Silicon Nitride
Speed rating (RPM)	70,000	85,000
Dynamic Load Rating (N)	8320	8320

Experimental Procedure

These initial tests were run at 17000 RPM to accelerate fault propagation, while avoiding rig resonances. Healthy tests were performed with each bearing at this speed with an axial load

applied such that the approximate maximum contact stress in the bearing was 1.90 GPa (275 ksi). While radial load is possible with the current setup, the radial load cylinder was neither used nor installed for these particular tests. The healthy tests were continued for 3-5 hours to ensure the equipment was at a steady state temperature and to allow for a run-in period. Vibration data was collected for one second every thirty seconds during both healthy and seeded fault tests. Between data acquisition intervals, the data was processed to calculate several vibration-based condition indicators to allow for damage trending during testing.

Following the completion of the healthy test, the bearing was removed and disassembled. The inner race was cleaned and a fault was seeded in the wear track with a Rockwell indenter using a special bearing fixture. This fixture supported the bearing during indentation such that the indenter was centered on and normal to the inner race wear track. The bearing was then reassembled and reinstalled in the rig. Testing then continued under the same conditions as the healthy test and damage was propagated until approximately 12 mg of ferrous debris passed through the debris sensor, after which the test was completed and the bearing was removed, disassembled and photographed. In the event that damage failed to propagate in a timely fashion under the specified loading, the axial load was increased on occasion until particles were generated and then returned to the original loading condition.

Results

An overview of the data recorded during both hybrid and conventional tests is shown below including the axial load and root mean square (RMS) of the test housing vibration alongside the approximate ferrous debris mass (Fig. 3). The most noticeable difference between the hybrid (Fig. 3a) and conventional (Fig. 3b) test is the overall run time. The first test performed, the hybrid test, continued for far longer than the conventional test. The initial seeded fault test (from approximately hour 4 to hour 8) acquired little to no damage on the bearing despite long durations at elevated loading. It was also noted during this test that no increase in oil outlet temperature was experienced until a significantly higher load was applied. This suggested the presence of some secondary load path in the equipment. At this point, the test was stopped and the test section was examined.

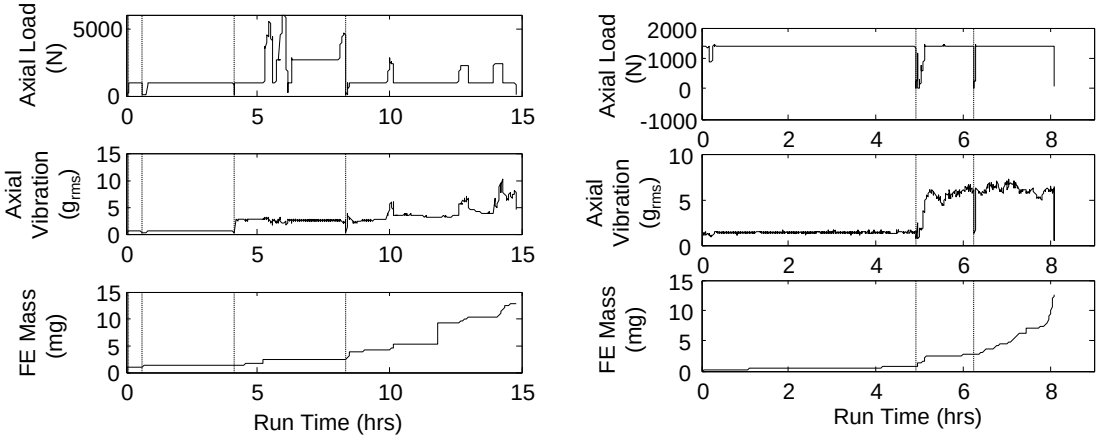

Fig. 3: Test data for both a) hybrid bearing, b) conventional bearing

Upon closer examination, a large amount of endplay was discovered in the shaft while under a significant static axial load, further verifying the presence of a 2nd load path. Test bearing

position was adjusted by shifting the bearing location on the shaft to ensure proper loading. A simplified view of the bearing housing is shown in Fig. 4a, with the intended load path identified. The bearing housing was designed to have a small gap between components. However, if the applied load takes up the available gap, the axial load bypasses the test bearing and travels into the housing of the adjacent support bearing (Fig. 4b). After the adjusting the test bearing shaft position, any increase from the normal loading condition caused an increase in the reaction thrust bearing oil outlet temperature, suggesting an applied axial load. Despite this adjustment, some periods of increased loading were still required to propagate damage in the case of the hybrid bearing.

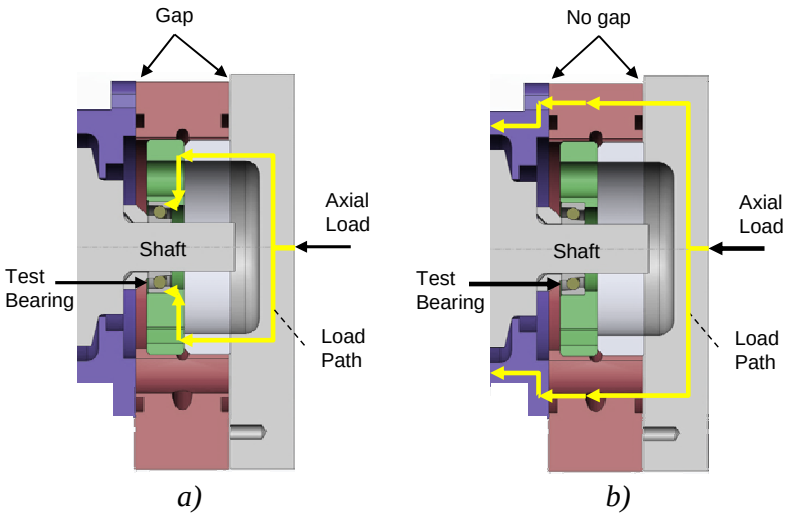

Fig. 4: Load path diagram: a) with gap between ram plate and bearing housing, b) without gap.

Short time fast fourier transforms of the vibration data from each test are shown in Fig. 5 for both the hybrid and conventional tests. Both healthy and seeded fault runs are shown here using the run time displayed in Fig. 3. These plots allow for the progression of damage to be viewed in the frequency domain. The first few shaft orders are shown here as well as the inner race ball pass frequency and the first few associated harmonics. The inner race ball pass frequency (BPFI) can be calculated using the method described in [10]. For these test bearings at a run speed of 17000 RPM (~283 rev/sec), the BPFI comes to approximately 2319 Hz. In both cases, damage is evident earlier in the BPFI harmonics than the BPFI itself. As damage progresses, it is also evident that the sidebands around the BPFI harmonics, generally at the shaft frequency, increase.

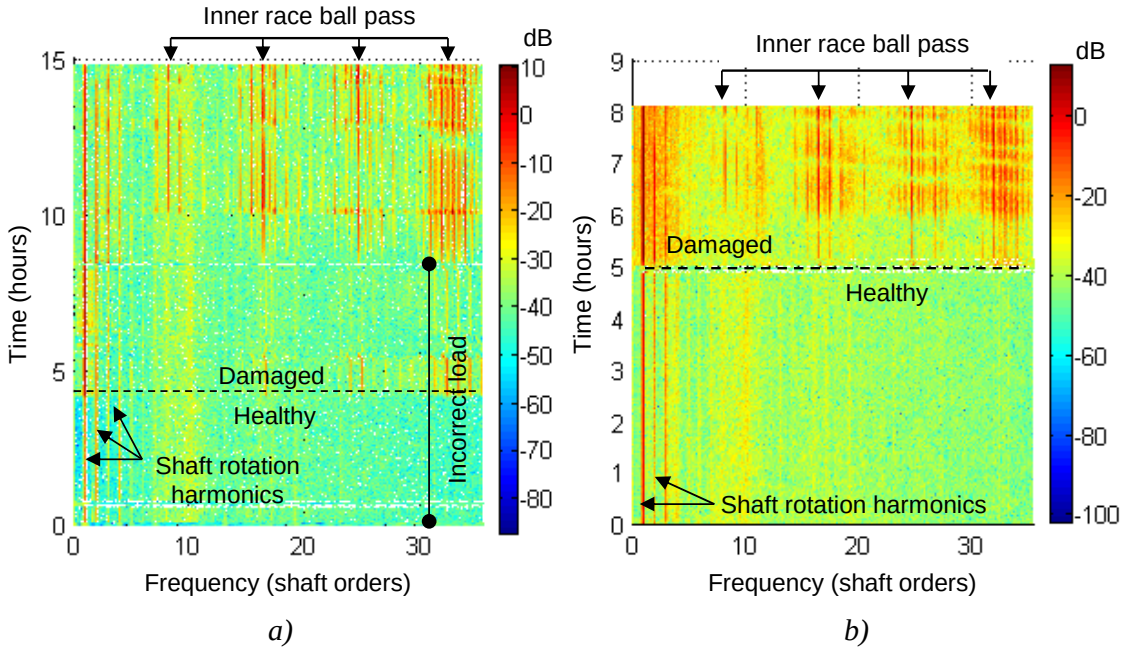

Fig. 5: Axial vibration magnitude over time: a) hybrid bearing, b) conventional bearing

Photographs of the resulting damage on both bearings can be viewed in Fig. 6. Examining closely, the original seeded fault is still visible in both photographs on the right side. In the hybrid case (Fig. 6a), the indenter mark is approximately a ¼ way from the right hand side. In the case of the conventional bearing (Fig. 6b), the mark is very near the right edge of the spall. For both cases, the rolling elements would have been traversing the inner race from right to left.

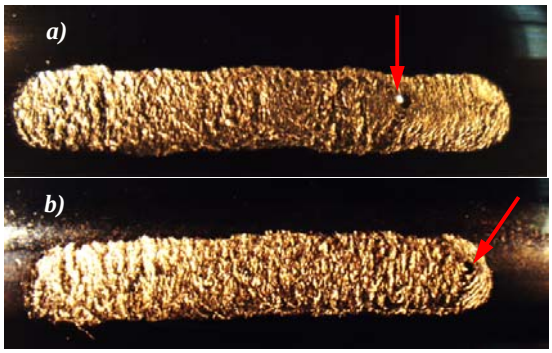

Fig. 6: Photograph of inner race bearing: a) hybrid bearing, b) conventional bearing

The fault frequency and its harmonics are seen in the frequency spectra shown in Fig. 7 with sidebands at the shaft frequency. The BPFI and associated harmonics and sidebands appear to be stronger in the case of the hybrid bearing. The conventional bearing test had significantly higher overall bearing housing vibrations during seeded fault testing, which made reaching the planned run condition difficult without unintentional shutdown. Examining the data, this test experienced more content at the lower frequencies than the hybrid seeded fault test. In particular, a quarter shaft frequency vibration with harmonics. This is currently expected to be caused by some mechanical looseness in the rig specific to the seeded fault portion of the conventional bearing test. Further testing would be required to confirm.

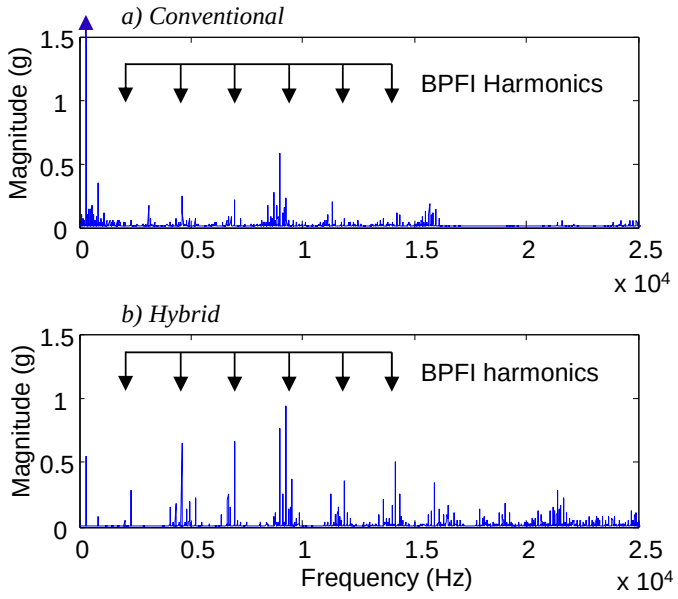

Fig. 7: Faulted vibration spectrum for an a) conventional and b) hybrid bearing

The bearing energy condition indicator (CI) is one used in the Army's rotorcraft fleet for bearing diagnostics. This CI measures the vibration energy in a certain band. The band generally is set to encompass the bearing fault frequencies while avoiding shaft frequencies and gear mesh frequencies [11]. In this case, the band from 1000 to 5000 Hz was chosen. This excludes the first few shaft orders while including the inner race fault frequency along with one harmonic. Results for both tests are displayed in Fig. 8. In each case, the bearing energy condition indicator indicates damage, though the indicator is not always increasing.

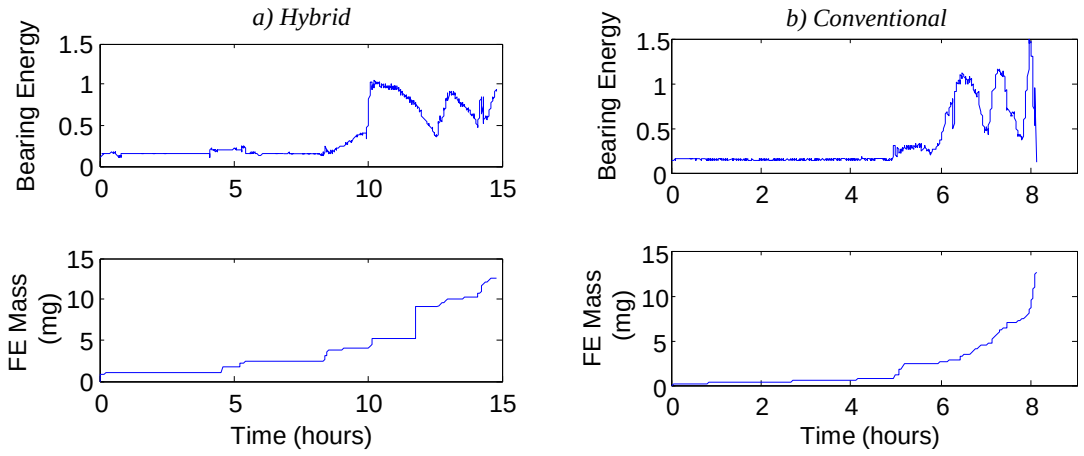

Fig. 8: Bearing energy condition indicator: a) hybrid, b) conventional

Conclusions

A preliminary look at high speed conventional and hybrid bearing fault signatures has been presented. A seeded fault test was performed for both a conventional steel bearing and a hybrid bearing with silicon nitride rolling elements. Although these two seeded fault tests suggest that inner race faults in hybrid bearings would be identified using currently available

methods and sensors, there are limitations to the results presented. First, the tests presented identified that there is potential for multiple load paths with the current test bearing housing design. This stems from a complicated test section design meant to allow both radial and axial load to be applied while keeping the test bearing and support system lubrication systems separate. Second, the rig was designed specifically such that the test bearing is the only rolling element bearing in the test section. This results in a clean vibration environment without the additional noise of meshing gears and other rolling element bearings, which could affect the ability to identify faults in either bearing type. It is difficult to make any generalized conclusions based on a single pair of tests. The author hopes to perform additional tests with an updated bearing housing design to further examine the vibrations of these bearings under this and other fault modes.

Acknowledgements

The author would like to acknowledge the NASA Glenn Research Center for the use of their facilities. The author would also like to acknowledge the support of Glenn Research Center technicians Roger Tuck and Sigurds Lauge for their assistance.

References

1. Gmirya, Y., et al., "Design and Analysis of 5100 HP RDS–21 Demonstrator Gearbox." Proceedings of the American Helicopter Society 60th Annual Forum, Baltimore, MD, 2004.

2. Hamrock, Bernard J. *Fundamentals of Fluid Film Lubrication.* NASA Technical Report. Columbus, OH: Ohio State University, 1991.

3. Chavez, Andrea, Jason Fetty, and Joseph Gerardi. 2014. "Non-Metallic Debris Monitor for a Helicopter Transmission." In *Proceedings of the 70th Annual Forum of the American Helicopter Society International, Inc.*, Montreal, Canada, May 20-22, 2014.

4. Ohta, H., and K. Kobayashi. "Vibrations of Hybrid Ceramic Ball Bearings." *Journal of Sound and Vibration*, Vol. 192, No. 2, 1996, pp. 481–93.

5. Ohta, Hiroyuki, and Shinya Satake. "Vibrations of the All-Ceramic Ball Bearing." *Journal of Tribology,* Vol. 124, No. 3, 2002, pp. 448-460.

6. He, David, Ruoyu Li, Mikhail Zade, and Junda Zhu. "Development and Evaluation of AE Based Condition Indicators for Full Ceramic Bearing Fault Diagnosis." *Conference Proceedings of the 2011 Prognostics and Health Management,* IEEE, Montreal, Canada, June 2011.

7. He, D., Ruoyu Li, Junda Zhu, and M. Zade. "Data Mining Based Full Ceramic Bearing Fault Diagnostic System Using AE Sensors." *IEEE Transactions on Neural Networks.* Vol. 22, No. 12, 2011, pp. 2022–31.

8. Dempsey, P. J., J. M. Certo, and R. F. Handschuh. "Hybrid Bearing Prognostic Test Rig." Proceedings of *2005 Annual Meeting and Exhibition,* Society of Tribologists and Lubrication Engineers, Las Vegas, NV, May 2005.

9. SKF Super-precision bearings, catalog 13383-EN, SKF Group, 2014.

10. Howard, Ian. 1994. *A Review of Rolling Element Bearing Vibration: Detection, Diagnosis and Prognosis*. Research Report DSTO-RR-0013, Defence Science and Technology Organisation, Melbourne, Australia, 1994.

11. *Aeronautical Design Standard Handbook: Condition Based Maintenance System for US Army Aircraft*, ADS-79D, US Army Aviation and Missile Research Development and Engineering Center, Redstone Arsenal, AL, 2013.